KeAi
CHINESE ROOTS
GLOBAL IMPACT

Available online at www.sciencedirect.com

ScienceDirect

Advances in Climate Change Research 11 (2020) 172−184

www.keaipublishing.com/en/journals/accr/

Risks of temperature extremes over China under 1.5 °C and 2 °C global warming

SHI Chen[a,b], JIANG Zhi-Hong[b,*], ZHU Lian-Hua[c], Xuebin ZHANG[d], YAO Yi-Yi[c], Laurent LI[e]

[a] *Laboratory of Research for Middle-High Latitude Circulation System and East Asian Monsoon, Jilin Provincial Key Laboratory of Changbai Mountain Meteorology & Climate Change, Institute of Meteorological Sciences of Jilin Province, Changchun, 130062, China*

[b] *Key Laboratory of Meteorological Disaster of Ministry of Education, Joint International Research Laboratory of Climate and Environment Change, Collaborative Innovation Center on Forecast and Evaluation of Meteorological Disaster, Nanjing University of Information Science & Technology, Nanjing, 210044, China*

[c] *School of Mathematics and Statistics, Nanjing University of Information Science & Technology, Nanjing, 210044, China*

[d] *Climate Research Division, Environment and Climate Change Canada, Toronto, Ontario M3H 5T4, Canada*

[e] *Laboratoire de Météorologie Dynamique, CNRS, Sorbonne Université, Ecole Normale Supérieure, Ecole Polytechnique, Paris, 75005, France*

Received 6 August 2020; revised 3 September 2020; accepted 9 September 2020
Available online 18 September 2020

Abstract

The Paris Agreement aims to keep global warming to well below 2 °C above pre-industrial levels and to pursue efforts to limit it to 1.5 °C, recognizing this will reduce the risks of natural disasters significantly. As changes in the risks of temperature extremes are often associated with changes in the temperature probability distribution, further analysis is still needed to improve understanding of the warm extremes over China. In this study, changes in the occurrence probability of temperature extremes and statistic characteristics of the temperature distribution are investigated using the fifth phase of the Coupled Model Intercomparison Project (CMIP5) multimodel simulations from 1861 to 2100. The risks of the once-in-100-year TXx and TNx events are projected to increase by 14.4 and 31.4 times at 1.5 °C warming. Even, the corresponding risks under 2 °C global warming are 23.3 and 50.6, implying that the once-in-100-year TXx and TNx events are expected to occur about every 5 and 2 years over China, respectively. The Tibetan Plateau, Northwest China and south of the Yangtze River are in greater risks suffering hot extremes (both day and night extremes). Changes in the occurrence probability of warm extremes are generally well explained by the combination of the shifts in location and scale parameters in areas with grown variability, i.e., the Tibetan Plateau for TXx, south of the Yangtze River for both TXx and TNx. The location (scale) parameter leading the risks of once-in-20-year TXx to increase by more than 5 (0.25) and 3 (0.75) times under 2 °C warming in the Tibetan Plateau and south of the Yangtze River, respectively. The location parameter is more important for regions with decreased variability e.g., the Tibetan Plateau for TNx, Northwest China for both TXx and TNx, with risks increase by more than 3, 6 and 4 times due to changes in location.

Keywords: 1.5 °C and 2 °C global warming; Temperature extremes; Risk ratios; GEV; CMIP5

1. Introduction

In December 2015, the 21st Conference of the Parties (COP 21) in Paris under the United Nations Framework Convention on Climate Change (UNFCC) proposed a long term goal to keep global warming to well below 2 °C and to pursue efforts to limit global mean temperature increase to 1.5 °C (UNFCCC, 2015). In the statement released by the World

* Corresponding author.
E-mail address: zhjiang@nuist.edu.cn (JIANG Z.-H.).

Peer review under responsibility of National Climate Center (China Meteorological Administration).

https://doi.org/10.1016/j.accre.2020.09.006

Meteorological Organization (WMO) recently, 2019 is the 2nd warmest year on record with global mean temperature increased by 1.1 ± 0.1 °C relative to pre-industrial levels and the past five years (2015−2019) are the five warmest in instrumental records (WMO, 2020). As the global mean temperature increase is getting closer to the 1.5 °C target, there is growing urgency to conduct research to understand the impacts and detrimental effects of climate change at the two warming targets for different regions (or countries) of the world.

China is a vulnerable area to global warming as a result of its prominent monsoon climate and complex topography (Huang et al., 2013). Most previous studies on the topic have been carried out regarding the 2 °C warming target in China (Jiang et al., 2009; Jiang and Fu, 2012; Lang and Sui, 2013; Sui et al., 2015, 2018). Within the framework of the Paris Agreement that went into force in November 2016, a growing body of literature has focused on the 1.5 °C warming target, especially the 0.5 °C difference between the two warming levels. Under the 1.5 °C and 2 °C targets, mean temperature over China would respectively increase by 1.7−2 °C and 2.4−2.7 °C relative to pre-industrial levels, with stronger increase in Northwest China (Jiang et al., 2009; Jiang and Fu, 2012; Lang and Sui, 2013; Fu et al., 2018; Shi et al., 2018; Sun et al., 2019; Yin et al., 2020). The total precipitation is projected to increase 7% and 11% in eastern China under 1.5 °C and 2 °C global warming (Li et al., 2020), and the number of days for heavy rain (>10 mm) might increase by 12% over eastern regions as a result of the additional 0.5 °C warming (Guo et al., 2019). Regarding hot extremes, even small changes in global mean temperature could lead to much more important and significant regional changes (Knutti et al., 2016). For the additional 0.5 °C warming, for example, increases in the hottest day (TXx) and coldest night (TNn) might be larger than 1 °C in Northwest China, Northeast China and over the Tibetan Plateau (Guo et al., 2018; Shi et al., 2018). The impacts of the extreme heat events are projected to increase by 53%−84% and 53%−107% in Northeast China and Northwest China, respectively, due to the additional 0.5 °C warming (Zhang et al., 2020).

Global warming affects not only the intensity of extremes, but also their probability or frequency of occurrence. It generally increases the risk of extreme warm events and decreases that of extreme cold events (IPCC, 2013). Under 1.5 °C and 2 °C global warming, the occurrence probability of once-in-20-year TXx is projected to increase about 130% and 340%, respectively (Kharin et al., 2018).For China, the additional 0.5 °C global warming would lead to an extra increase in the risk of extreme events by 4.1 times relative to 1986-2005 (Yu et al., 2018). Also, for heat waves like the historically hottest summer in 2013 over eastern China which caused substantial social and economic damages, the once-in-5-year event in the 2013 climate is projected to become a once-in-2-year event under 1.5 °C global warming and almost every year event under an additional 0.5 °C warming (Sun et al., 2018).

In recent years, a number of studies have sought to identify possible factors that affect the changes in temperature extremes based on observations and model outputs. For example, using station-based data, Parey et al. (2013) presented evidence that changes in temperature extremes over Eurasia and the United States closely follow the changes in means and standard deviations of the temperature distributions. Donat and Alexander (2012) also pointed out that changes in the temperature extremes (both daytime and nighttime) are associated with shifts in multiple aspects of temperature distributions rather than just changes in the mean. In contrast, Rhines and Huybers (2013) argued that frequent summer temperature extremes reflect mainly changes in the mean, but not very much in the variance of the temperature distribution. A more recent study suggests that changes in the distribution of daily minimum and maximum surface air temperature in the Northern Hemisphere mid-latitudes are largely (87%−88% of the stations) associated with a positive shift in the distributions without changes in the shape (McKinnon et al., 2016). In summary, it is still a highly-controversial issue to understand how the mean and variability contribute to changes in temperature extremes, especially in studies that focus on risks based on occurrence probability in the tail of the distribution or so called risk ratios (e.g., Fischer and Knutti, 2015; Frölicher and Laufkötter, 2018; Kharin et al., 2018; Li et al., 2018a). We want to revisit this issue in China under the context of global warming at 1.5 °C and 2 °C levels. Our approach will be based on the investigation of parameters entering into the mathematical functions used to describe extreme events in a probabilistic way. Such parameters with their precise physical significance can help us to deepen our understanding on the physical background of extreme events.

Extreme value theory (EVT) is widely used to explore the changes in extreme climate events (Easterling et al., 2000; Kharin et al., 2007, 2013, 2018; Lee et al., 2014; Li et al., 2018b; Zhu et al., 2017) and one common approach is the generalized extreme value (GEV) distribution. GEV has also been applied to a few studies regarding the Paris Agreement. Kharin et al. (2018), for instance, made use of GEV to evaluate the differences in the risks of temperature extremes and precipitation extremes between two warming limits. Similarly, based on GEV, Li et al. (2018a, 2018b) found that the probability of a once-in-100-year historical extreme precipitation event over 1986−2005 in China will increase 1.6 and 2.4 times under 1.5 °C and 2 °C global warming, respectively. However, there are relatively few studies that investigate the influence of 1.5 °C or 2 °C global warming on the different parameters (location, scale and shape parameters) of GEV distribution, which ultimately affect the occurrence probability (or risk) of temperature extremes. To address this question, further analysis is still needed to understand the possible changes in future temperature extremes beyond simply assessing the changing magnitude of extreme temperature events. Therefore, we focus on the contribution of different GEV parameters to the

occurrence probability of temperature extremes at 1.5 °C and 2 °C warming levels in China, based on the fifth phase of the Coupled Model Intercomparison Project (CMIP5) multimodel simulations. The results can provide theoretical foundation to the emission reduction and adaptation strategies for Chinese government.

2. Data and methods

2.1. Data

Daily minimum and maximum temperatures are extracted from 14 CMIP5 models (Table 1), including historical simulation for the period 1861−2005 as well as future projections under the RCP8.5 (Representative Concentration Pathways) scenario for the period 2006−2100. We selected these 14 models by only considering the availability of their outputs. As results are quite independent of precise RCP scenarios leading to the global warming levels at 1.5 °C or 2 °C (not shown), only the results derived from RCP8.5 are shown in the present study. The historical simulation was realized with both natural (solar irradiance and volcanic activity) and anthropogenic forcings. RCP8.5 represents the highest emission scenario and it is actually the most representative of global CO_2 emissions from 2005 to present (Peters et al., 2013). All the analyses are based on the first realization of each model in order to treat all models equally.

We also used monthly outputs of historical and RCP8.5 experiments from the 14 models mentioned above to determine the timing of 1.5 °C and 2 °C warming thresholds. We used years 1861−1900 to represent the pre-industrial level, which is a period with smaller human influence and a commonly available time interval for CMIP5 models (Shi et al., 2018; Guo et al., 2020). Then we smoothed the time series of global mean temperature anomalies (relative to 1861−1900) of each model by a 21-year moving average to suppress the interannual variability. The first year when the temperature increase reaches 1.5 °C or 2 °C determines the time window with 10 years forward and 10 years backward.

Table 1
Basic information of 14 CMIP5 models used in this study.

Model	Model center	Horizontal resolution (latitude × longitude)
BCC-CSM1.1	BCC-CMA, China	128 × 64
CanESM2	CCCMA, Canada	128 × 64
CCSM4	NCAR, America	288 × 192
CSIRO-MK3-6-0	CSIRO-QCCCE, Australia	192 × 96
CNRM-CM5	CNRM-CERFACS, France	256 × 128
GFDL-CM3	NOAA GFDL, America	144 × 90
GFDL-ESM2M	NOAA GFDL, America	144 × 90
HadGEM2-ES	MOHC, UK	192 × 145
IPSL-CM5A-LR	IPSL, France	96 × 96
IPSL-CM5A-MR	IPSL, France	144 × 143
MIROC-ESM	MIROC, Japan	128 × 64
MIROC-ESM-CHEM	MIROC, Japan	128 × 64
MRI-CGCM3	MRI, Japan	320 × 160
NorESM1-M	NCC, Norway	144 × 96

2.2. Methodology

2.2.1. Extreme temperature indices

Two extreme temperature indices are considered following the recommendation of Expert Team on Climate Change Detection and Indices (ETCCDI) (Zhang et al., 2011). They are annual maximum of daily maximum temperature (TXx) and annual maximum of daily minimum temperature (TNx). Both the indices are calculated on the native grid of individual models based on CMIP5 daily outputs.

2.2.2. Probability ratio to measure variation of risks

The probability ratio (PR) is defined as follows (Stott et al., 2004, 2016; Fischer and Knutti, 2015): $PR = P_1/P_0$, where P_0 is the probability of an event (e.g., TXx and TNx) higher than a threshold under historical simulations and P_1 is the probability higher than the same threshold under future simulations, for instance, at 1.5 °C or 2 °C warming level. If $PR > 1$, it implies that global warming has increased the risk of historical events in the future warming.

2.2.3. GEV distributions and derivations

To investigate the influence of different parameters, a GEV distribution is first fitted to a sample of annual temperature extremes. The cumulative distribution function (CDF), described in terms of its three parameters (Coles, 2001), is

$$G(x;\mu,\sigma,\xi)=\exp\left\{-\left[1+\frac{\xi(x-\mu)}{\sigma}\right]_+^{-\frac{1}{\xi}}\right\},\ \sigma>0,\ 1+\frac{\xi(x-\mu)}{\sigma}>0 \quad (1)$$

where μ is the location parameter, σ is the scale parameter, and ξ is the shape parameter. Changes in the different GEV parameters can have different impacts on the distributions of annual extremes. Generally, the distribution of annual extremes is shifted with the change $\Delta\mu$ by simply changing the location parameter μ. Changing the scale parameter σ affects the variability of the distribution of annual extremes, in other words, increasing (decreasing) σ broadens (narrows) the distribution. Changing the shape parameter ξ influences the symmetry in the distribution of annual extremes, by altering the tail behavior of the distribution. We have verificated the fitted GEV distribution and the empirical one to ensure its reliability in fitting the distribution of TXx and TNx (results not shown).

It should be clear that although the scale and shape parameters both affect the variability of extreme temperature distribution, we considered scale parameter as the only factor controlling the variability hereafter due to relatively small changes in the shape parameter (results not shown), but consistent with those presented in Goubanova and Li (2007) for the Mediterranean area. Consequently, to better convey the impacts of different parameters on the risks, here we assumed shape parameter ξ stay constant for a specific warming level and make the following derivation. Consider two GEV distributions, described as $X \sim G(\mu_0, \sigma_0, \xi_0)$ and

$X' \sim G(\mu,\sigma,\xi_0)$, where $\mu = \mu_0 + \Delta\mu$ and $\sigma = \sigma_0 + \Delta\sigma$. Then the probability ratio (PR) can be expressed as

$$\begin{aligned} PR &= \frac{P_1}{P_0} = \frac{1-P(X' \le x_{P_0})}{1-P(X \le x_{P_0})} = \frac{1-G(x_{P_0})}{P_0} \propto 1-G(x_{P_0};\mu,\sigma,\xi_0) \\ &= 1-\exp\left\{-\left[1+\frac{\xi_0(x_{P_0}-\mu)}{\sigma}\right]^{-\frac{1}{\xi_0}}\right\} = 1-\psi\left(\frac{x_{P_0}-\mu}{\sigma}\right) \\ &= PR(\mu,\sigma) \end{aligned} \tag{2}$$

To satisfy differentiable conditions, denote $\mu = k_\mu \mu_{\max}$ and $\sigma = k_\sigma \sigma_{\max}$, respectively. Then the PR due to shift in location parameter μ and scale parameter σ can be written as

$$PR_{k_\mu} = 1-\psi\left(\frac{x_{P_0}-k_\mu\mu_{\max}}{\sigma_0}\right) \tag{3}$$

$$PR_{k_\sigma} = 1-\psi\left(\frac{x_{P_0}-\mu_0}{k_\sigma\sigma_{\max}}\right) \tag{4}$$

where $\mu_{\max}/\sigma_{\max}$ is the maximum location/scale parameter of historical and 1.5 °C or 2 °C warming level, and k is the rate of corresponding parameter. The derivation functions of Eqs. (3) and (4) should be

$$\begin{aligned} PR'_{k_\mu} &= [(1-G(x_{P_0};k_\mu\mu_{\max},\sigma_0,\xi_0))]'_{k_\mu} = -G(x_{P_0};k_\mu\mu_{\max},\sigma_0,\xi_0)'_{k_\mu} \\ &= -\exp\left\{-\left[1+\frac{\xi_0(x_{P_0}-k_\mu\mu_{\max})}{\sigma_0}\right]^{-\frac{1}{\xi_0}}\right\}'_{k_\mu} \\ &= \exp\left\{-\left[1+\frac{\xi_0(x_{P_0}-k_\mu\mu_{\max})}{\sigma_0}\right]^{-\frac{1}{\xi_0}}\right\}. \\ &\quad \left\{\left[1+\frac{\xi_0(x_{P_0}-k_\mu\mu_{\max})}{\sigma_0}\right]^{-\frac{1}{\xi_0}-1}\right\}\cdot\frac{\mu_{\max}}{\sigma_0} \end{aligned} \tag{5}$$

$$\begin{aligned} PR'_{k_\sigma} &= [(1-G(x_{P_0};\mu_0,k_\sigma\sigma_{\max},\xi_0))]'_{k_\sigma} = -G(x_{P_0};\mu_0,k_\sigma\sigma_{\max},\xi_0)'_{k_\sigma} \\ &= -\exp\left\{-\left[1+\frac{\xi_0(x_{P_0}-\mu_0)}{k_\sigma\sigma_{\max}}\right]^{-\frac{1}{\xi_0}}\right\}'_{k_\sigma} \\ &= \exp\left\{-\left[1+\frac{\xi_0(x_{P_0}-\mu_0)}{k_\sigma\sigma_{\max}}\right]^{-\frac{1}{\xi_0}}\right\}. \\ &\quad \left\{\left[1+\frac{\xi_0(x_{P_0}-\mu_0)}{k_\sigma\sigma_{\max}}\right]^{-\frac{1}{\xi_0}-1}\right\}\cdot\left(\frac{x_{P_0}-\mu_0}{k_\sigma^2\sigma_{\max}}\right) \end{aligned} \tag{6}$$

Here, we define PR'_{k_μ} and PR'_{k_σ} as the variation rate of the risks induced by location and scale parameter, respectively. A larger PR'_{k_μ} or PR'_{k_σ} indicates more rapid changes in the risks for a specific parameter.

Hence, the total differential equation can be expressed as

$$dPR = PR'_{k_\mu}dk_\mu + PR'_{k_\sigma}dk_\sigma \tag{7}$$

where $PR'_{k_\mu}dk_\mu$ and $PR'_{k_\sigma}dk_\sigma$ are defined as contribution rates which mean the changes in risks caused by location parameter and scale parameter hereafter, respectively.

2.2.4. Model fitting procedures

For studying high temperature extremes, the three parameters in Eq. (1) are estimated on the native grid of each model under historical simulations and then the corresponding percentiles can be determined. Similarly, the GEV distribution at each grid box for the corresponding 1.5 °C or 2 °C global warming period under RCP8.5 simulations can also be fitted.

Having fitted the GEV distribution, the exceedance threshold under historical climate (i.e., 99th percentile for the once-in-100-year event) can be obtained on each grid box for respective model and the corresponding changes in occurrence probability of temperature extremes as well as the relevant variation/contribution rates for a given warming target can be estimated. In order to facilitate the comparison of different models, the PR and variation/contribution rates of individual models are regridded to a common 1° × 1° grid using bilinear interpolation. In this study, the geographical distribution of projected PR at a specific warming level is depicted as multimodel median values.

To deal with the information offered by the multimodel ensemble, we can use the ensemble median values for each of the three GEV parameters. That is, the estimated parameters of individual models, once obtained, are then interpolated onto a common 1° × 1° grid. Their median values are then taken as the reconstructed parameters to deduce the multimodel probability density functions (PDFs) and the PR associated. This alternative way to explore the multimodel ensemble at the level of GEV parameters is new and different from the primary way of using the multimodel ensemble information at the final level of PR. But the two approaches are quite close to each other and show consistent results. It is to be noted that the shape parameter ξ determines the precise mathematical form of the probability distribution, which forces us to exclude such models appearing in the category (ξ: <0, = 0, >0) minority of the ensemble. This situation, however, occurs very rarely, since the Weibull function ($\xi < 0$) seems the dominant case for us.

3. Results

3.1. Changes in the probability ratios of temperature extremes

Regional risk ratios are illustrated as a function of different return values (or different percentiles) under historical

conditions (1861−2005) (Fig. 1). The regional risk ratios are calculated by area-weighting PR on respective grids for individual models across China. Ultimately, 14 values of area-weighted PR can be obtained to form the box-plots in Fig. 1 for a specific warming level and return period. Consistent with previous studies (Fischer and Knutti, 2015; Kharin et al., 2018), PR for TXx and TNx with different return levels both increase under 1.5 °C and 2 °C global warming, indicating once again that global warming augments the risks of warm extremes. The PR differs substantially between the warming levels of 1.5 °C and 2 °C. For example, the corresponding median PR of TXx and TNx (expected once-in-100-year under historical conditions) at 1.5 °C global warming is 14.4 and 31.4, respectively, and a further 890% and 1920% increases for a 2 °C warming target (PR is 23.3 and 50.6). This also means that on average over China a TXx and TNx event expected every 100 years in historical simulations is expected about every 5 and 2 years under 2 °C global warming. There are substantial increases in the risks of TNx, with the median risks more than two times higher than TXx for a specific warming level and return value. The increases in PR are larger for a higher warming level and a higher percentile, which implies that global warming has greater influence on the occurrence probabilities of rarer extreme hot events. Furthermore, there is also a larger inter-model uncertainty range for a higher percentile.

Fig. 2 shows the spatial patterns of PR for TXx and TNx that occur once every 20 years under historical climate as compared to those at the two global warming levels. Under 1.5 °C and 2 °C global warming, the risks increase (PR > 1) across China, indicating more frequent occurrence of such hot extremes. There are very similar patterns between the 1.5 °C and 2 °C warming levels, whereas the latter has much larger values. In addition, there are substantial differences in the increasing magnitude across various regions. The PR for a historical once-in-20-year event is relatively higher in lower latitudes and higher altitudes (for instance, south of the Yangtze River the Tibetan Plateau, and Southwest China), with risks increasing by more than 10 and 20 times in these areas for TXx and TNx under 2 °C global warming, respectively. This means that these areas will have greater risks suffering hot extremes due to the influence of 1.5 °C and 2 °C global warming. The warming influence is more prominent in the changes of occurrence probability of TNx. This is due to the fact that TNx has a smaller variability which means a greater change in the probability for a similar temperature increase compared with TXx (Sun et al., 2016). Compared to 1.5 °C warming, for both TXx and TNx, PR is almost doubled over these areas under 2 °C global warming.

As for warm events expected to occur every 50 years, the risks are higher for the same warming level across China (results not shown). There are also larger differences between once-in-20-year and once-in-50-year events for a greater warming level. For example, the differences between the risk ratios of once-in-50-year and once-in-20-year events for TXx and TNx are 7 and 15 under 2 °C global warming, respectively, which are almost 2 times higher than that in a 1.5 °C warming level (Fig. 1).

3.2. Changes in the GEV parameters of temperature extremes

Relative to historical climate, there are greater variations of location parameter in the west of the Tibetan Plateau, Southwest China and Northwest China for TXx (Fig. 3a and b), with positive shifts of more than 2 °C and 2.5 °C at 1.5 °C and 2 °C warming levels, respectively. The scale parameter mainly increases in North China and south of the Yangtze River (Fig. 3c and d). There are differences in the sign of changes in scale parameter over Northeast China and western part of the Tibetan Plateau between the two global warming levels, with lower/higher variability under 1.5 °C/2 °C warming, implying that it might somewhat mitigate the warming rates at these same locations if global warming could be limited to 1.5 °C relative to pre-industrial levels.

The variation rate and contribution rate of location parameter and scale parameter are further calculated (Fig. 4). As the differences are very small between the two global warming levels, only the distributions of variation rate under 1.5 °C warming level are shown here. The variation rate of

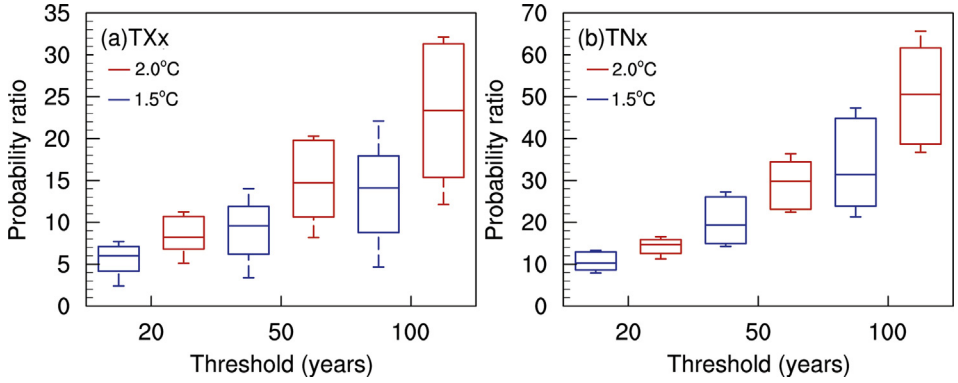

Fig. 1. Boxplots showing the distribution of multimodel probability ratios (relative to historical conditions (1861−2005), and averaged across China) for (a) TXx and (b) TNx exceeding the 95th (once-in-20-year), 98th (once-in-50-year) and 99th (once-in-100-year) percentiles under 1.5 °C and 2 °C global warming levels (The bottom and top whiskers are the 10th and 90th values. The bottom and top of boxes are the first and third quartiles, and the band inside the box is the median).

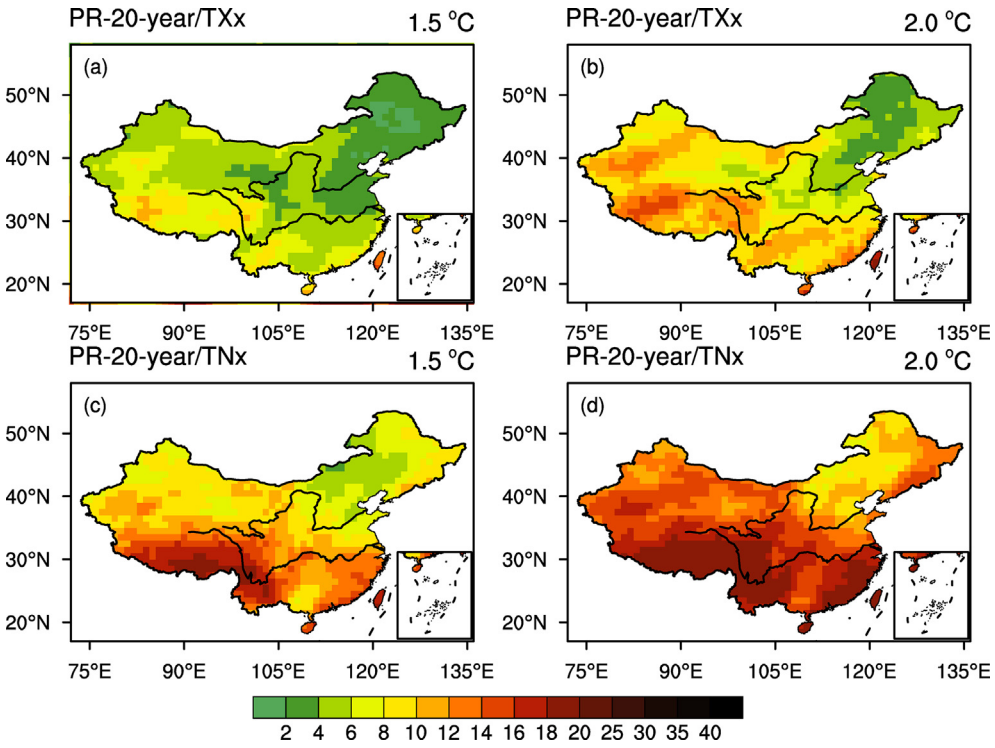

Fig. 2. Spatial distributions of probability ratios (expressed as multimodel median) for TXx and TNx that expected to occur every 20 years under 1.5 °C (a, c) and 2 °C (b, d) global warming levels.

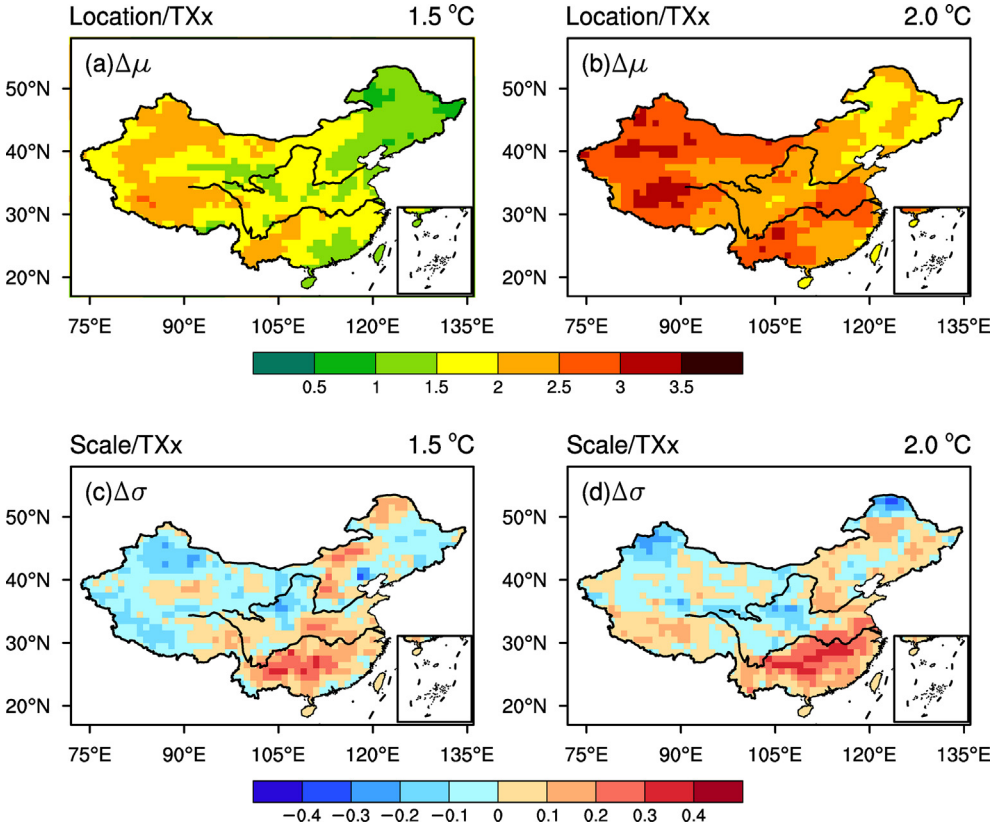

Fig. 3. Spatial distributions of the changes in (a, b) location μ and (c, d) scale σ (expressed as multimodel median) for TXx under 1.5 °C and 2 °C global warming levels.

location parameter is higher in Northwest China, Southwest China and southeast coastal areas (Fig. 4a), implying that the risks induced by changes in location parameter will increase faster over these regions under a specific warming level. As for scale parameter (Fig. 4b), greater variation rate is located in the west of the Tibetan Plateau and Southwest China. The change rates of the two GEV parameters are both positive which further proves that the risks of TXx increase with location parameter and scale parameter. In the south of the Yangtze River, there is greater contribution rate due to the higher variation rate of location and scale. The contribution rate is highest in the Tibetan Plateau due to the larger increases in location ($\Delta\mu$) and the greater variation rate of scale. This indicates that the variations of PR in the Tibetan Plateau and south of the Yangtze River are closely related to the combined effect of location and scale parameter. Relative to historical climate, under 2 °C global warming, the risks increase by more than 5 (0.25) and 3 (0.75) times in the Tibetan Plateau and south of the Yangtze River due to the impact of location (scale) parameter (Fig. 4d and f), respectively. While for

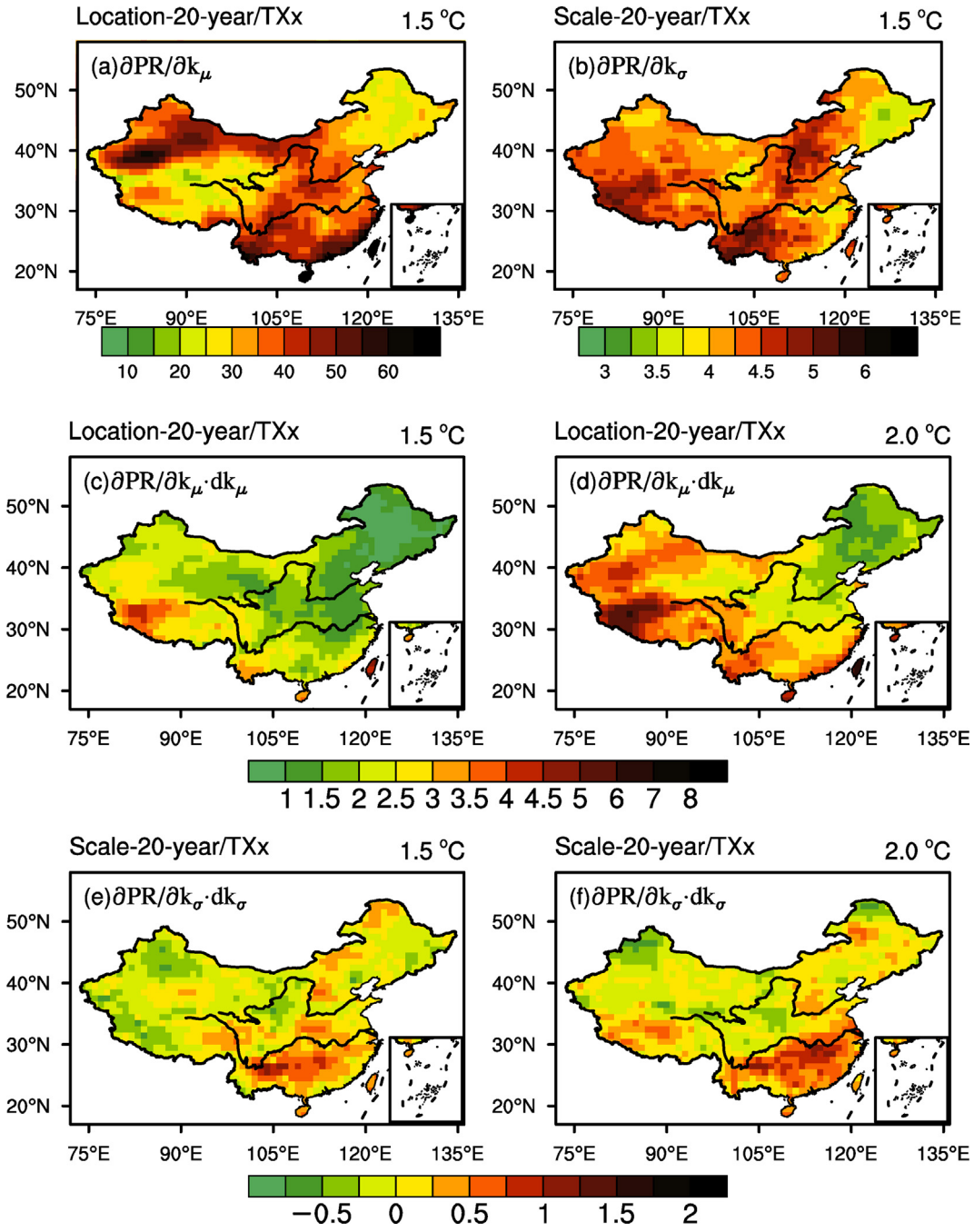

Fig. 4. Spatial distributions of the (a, b) derivations of probability ratios, and contribution rates in (c, d) location μ and (e, f) scale σ (expressed as multimodel median) for TXx expected every 20 years under 1.5 °C and 2 °C global warming levels.

Northwest China where there are also greater warming increments and decreased variability, the risks increase strongly but not so much as that in the Tibetan Plateau, suggesting that the relatively higher PR in Northwest China is mainly affected by the changes in location parameter. The location parameter is projected to lead the risks of a historical once-in-20-year event increase by more than 3 times in Northwest China, whereas the scale parameter is estimated to reduce the risks of about 0.5.

Figure 5 depicts the distribution of TNx in a manner similar to Fig. 3. The highest changes in location parameter of TNx are mainly situated in Northwest China (Fig. 5a and b), along with decreased variability. The variability of TNx mainly increases in mid-eastern China, with greater values in south of the Yangtze River (Fig. 5c and d).

Similar to TXx, the variation rate of location parameter is higher in south of the Yangtze River but with greater values, especially in southeastern part of Northeast China (Fig. 6a). The risks induced by the changes in scale parameter are positive across China and mainly increase in the Tibetan Plateau and Southwest China. Clearly, this again indicates that location parameter and scale parameter both promote to the increase in the risks of TNx. Although the variation rate of location parameter in the Tibetan Plateau is not the highest over China, the highest PR in the Tibetan Plateau is mainly attributable to the changes in location parameter due to the decrease in its variability (Fig. 6c and d). The risks in the Tibetan Plateau are projected to increase by more than 6 times relative to that in the historical climate under 2 °C global warming, as a consequence of the increases in location parameter. Similarly, next to the Tibetan Plateau, the location parameter contributes to the increases of risks in Northwest China, with the highest increments in location parameter and decreased variability under global warming over these grids. The risks are estimated to increase by more than 4 times relative to the historical climate at 2 °C warming. As for the areas in the south of the Yangtze River, the relatively higher risks are influenced by the combined effect of location parameter and scale parameter (Fig. 6d and f).

3.3. Changes in the probability distributions of temperature extremes

To provide more insight into the impacts of GEV parameters on the risks for warmest day and night temperature extremes, Fig. 7 displays the multimodel median GEV PDFs and the corresponding parameters over several grid points under historical, 1.5 °C and 2 °C warming level, respectively. There

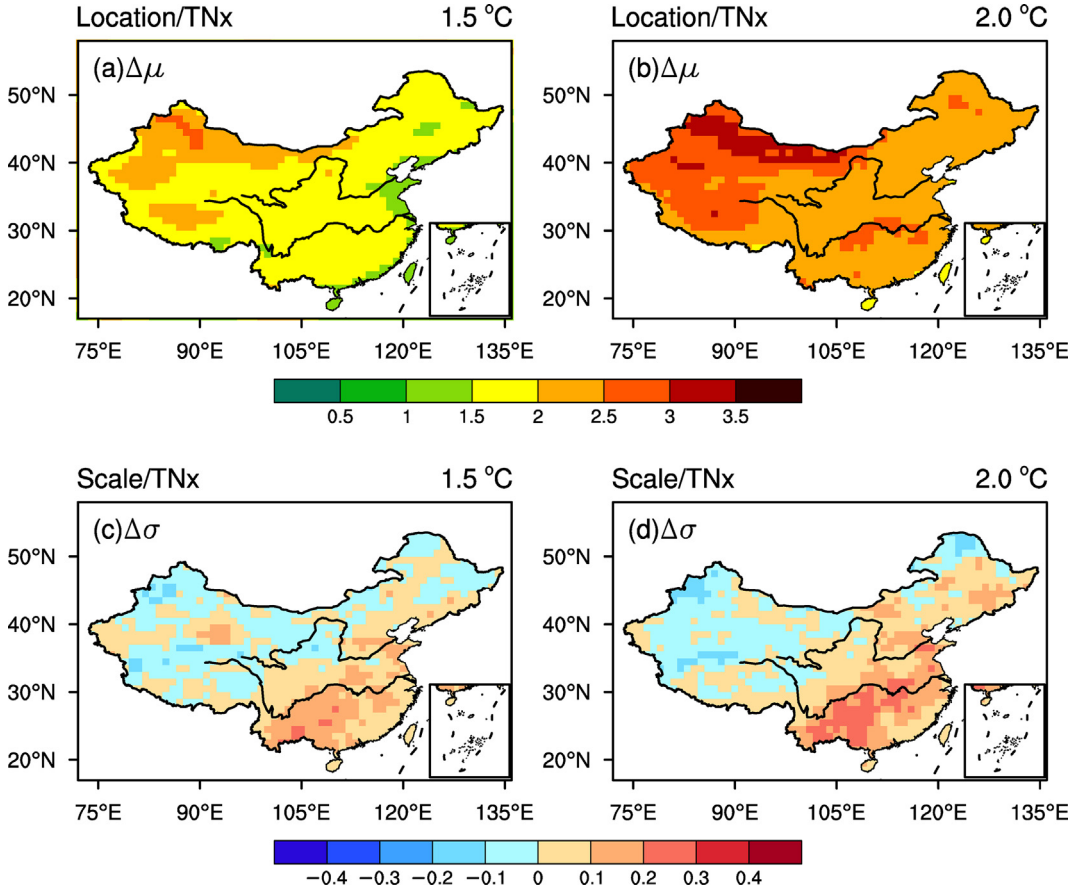

Fig. 5. Spatial distributions of the changes in (a, b) location μ and (c, d) scale σ (expressed as multimodel median) for TNx under 1.5 °C and 2 °C global warming levels.

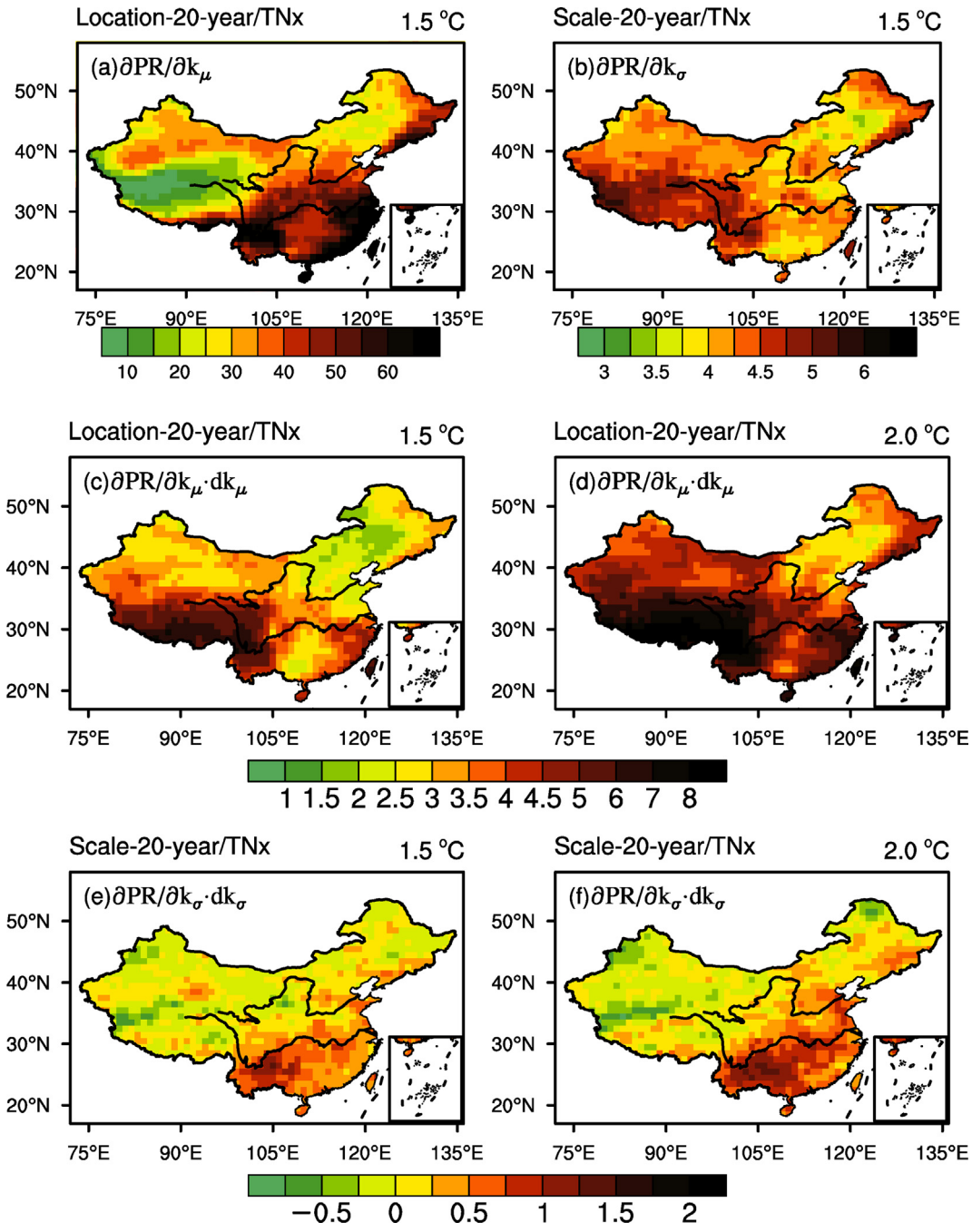

Fig. 6. Spatial distributions of the (a, b) derivations of probability ratios, and contribution rates in (c, d) location μ and (e, f) scale σ (expressed as multimodel median) for TNx expected every 20 years under 1.5 °C and 2 °C global warming levels.

is a clear positive shift in the location parameter for both TXx and TNx, indicating once again that global warming will increase the risks of warm temperature extremes. The shape parameter is negative over China, that is, the fitted PDF is a Weibull distribution, as is usually the case for temperature extremes (Huang et al., 2016; Zhang et al., 2017). In general, larger positive variations of location and scale parameter both contribute to increasing risks of TXx over areas such as Lhasa, Guangzhou and Shanghai, and the risks of a once-in-100-year TXx event are estimated to increase about 20 times (expected about every 5 years) under 2 °C warming (Table 2). Although the variability almost remains unchanged, among these six areas, Urumqi is the most sensitive location with the greatest warming increments of about 2.61 °C/3.16 °C under 1.5 °C/2 °C warming, i.e., a historical once-in-100-year TXx event is projected to occur about 20/30 times more frequently

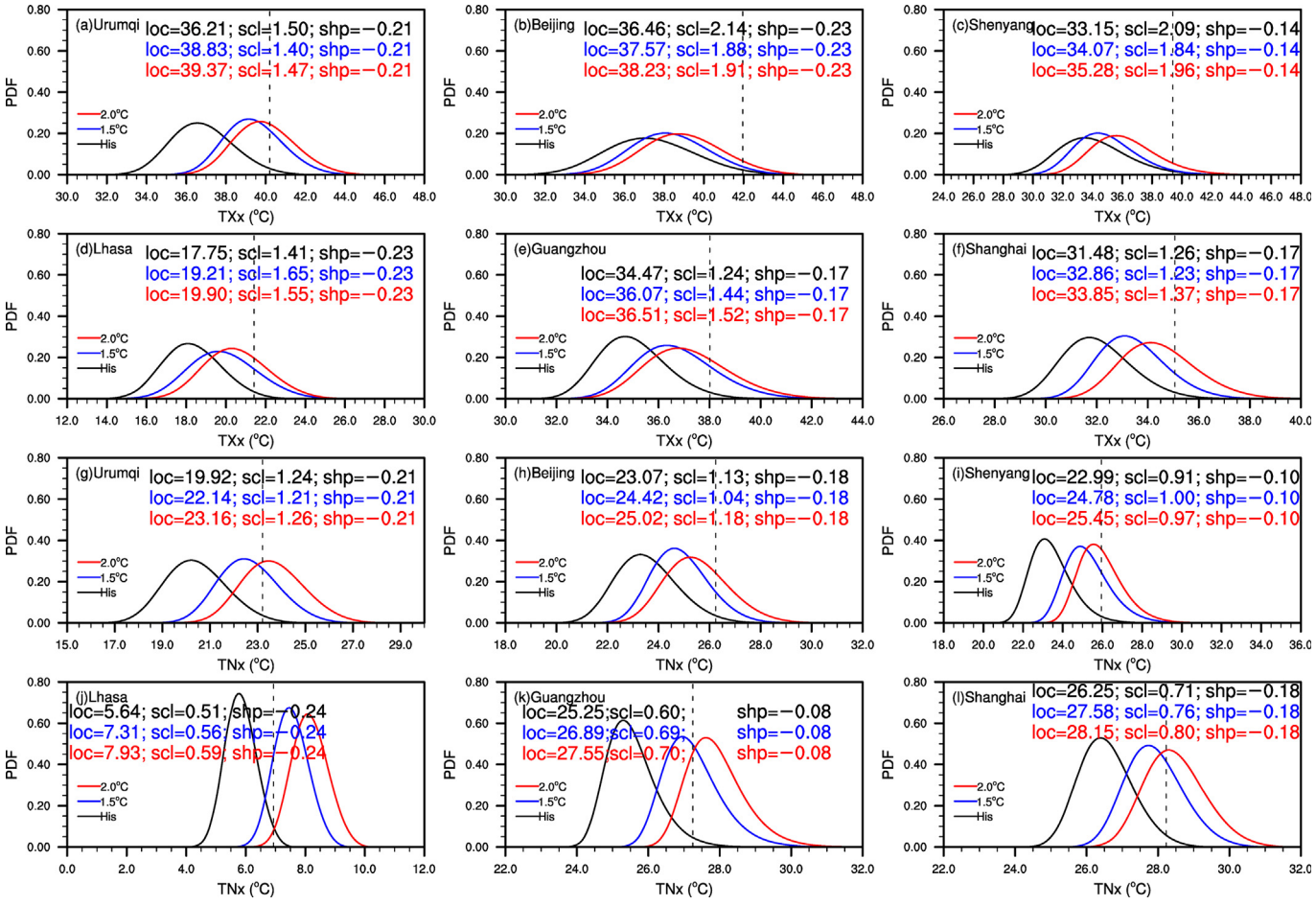

Fig. 7. Probability density functions (PDFs) satisfying GEV distributions for (top six panels, a−f) annual warmest day (TXx) and (bottom six panels, g−l) annual warmest night (TNx) for grid points corresponding to six emblematic cities, Urumqi, Beijing, Shenyang, Lhasa, Guangzhou and Shanghai (An independent GEV is used to fit each of the 14 climate models. The curves shown here are reconstructed with the three GEV parameters, 'loc' for location, 'scl' for scale, and 'shp' for shape, that take their values from the multimodel median. The vertical dashed lines represent the 98th percentiles (once-in-50-year return level) of the historical PDF curve).

(Table 2). Beijing and Shenyang is less sensitive to global warming due to the combined effect of smaller temperature increase and decreased variability, especially for Shenyang. For the other three cities, increased location and scale parameter both contribute to the greater risks under the two global warming levels. This further support the results mentioned above.

The width of the PDF distribution for TNx is narrower than that for TXx, which means that the variability of TNx is smaller than TXx. In other words, if the location parameter of TXx and TNx both increase 1 °C, there will be greater variations in the risk ratios of TNx. Under 2 °C global warming, for example, the risk for a once-in-100-year TNx event in Shenyang is projected to increase about 31 times (expected every 3 years), which is 2680% higher than that for a once-in-100-year TXx event (Table 2). In addition to the smaller variability of TNx, its variability also increases with global warming in Lhasa, Guangzhou, Shanghai and Shenyang, indicating the importance of the joint effect of location and scale parameters. However, for Urumqi and Beijing with reduced variability, the historical once-in-100-year TNx event is expected to occur almost every 2 and 5 years under 2 °C global warming (Table 2), respectively, as a result of greater warming amplitude in the location parameter.

In general, location parameter and scale parameter both contribute to the increase of risks for TXx over large areas where there is higher variability in the warmer world (i.e., mainly over the Tibetan Plateau, Southwest China and south of the Yangtze River). While for regions with lower variability, such as Northwest China, North China and Northeast China, location parameter plays a more important role in the changes of PR for TXx. Compared with TXx, in addition to the above two factors, higher risks of TNx are largely associated with its lower variability.

Table 2
Changes in location and scale parameters (reconstructed from the multimodel median values) as well as the corresponding return periods (expected every 20, 50 and 100 years in historical climate) under 1.5 °C and 2 °C global warming for TXx and TNx.

Station	Annual maximum of daily maximum temperature (TXx)						Annual maximum of daily minimum temperature (TNx)					
	Location		Scale		Return period (years, 1.5/2 °C)		Location		Scale		Return period (years, 1.5/2 °C)	
	his→1.5 °C	his→2.0 °C	his→1.5 °C	his→2.0 °C	20	50	100	his→1.5 °C	his→2.0 °C	his→1.5 °C	his→2.0 °C	20	50	100
Urumqi	2.61	3.16	−0.1	−0.04	2.2/1.7	3.5/2.4	5.0/3.1	2.22	3.24	−0.03	0.01	2.1/1.3	3.2/1.6	4.3/1.9
Beijing	1.11	1.77	−0.26	−0.23	11.9/6.6	29.5/13.9	59.0/24.2	1.35	1.95	−0.09	0.05	4.4/2.3	8.8/3.7	14.9/5.2
Shenyang	0.92	2.13	−0.24	−0.12	15.4/5.8	41.8/12.6	90.0/22.5	1.79	2.47	0.09	0.06	2.3/1.5	4.0/2.2	6.2/3.2
Lhasa	1.46	2.15	0.23	0.14	3.5/2.4	5.4/3.5	7.4/4.7	1.67	2.29	0.05	0.08	1.1/1.0	1.2/1.0	1.3/1.0
Guangzhou	1.6	2.04	0.2	0.29	3.2/2.4	5.1/3.5	7.3/4.7	1.65	2.31	0.09	0.09	1.5/1.1	2.2/1.3	3.2/1.6
Shanghai	1.38	2.37	−0.03	0.11	4.7/2.1	9.0/3.1	14.9/4.3	1.33	1.9	0.05	0.09	2.1/1.3	3.1/1.7	4.2/2.1

4. Conclusions

Widespread climate extreme events may affect the most populous and prosperous regions in China and produce substantial impacts on humans and ecosystems, it is crucial to understand the statistical characteristics of changes in the climate extremes. Based on CMIP5 multimodel simulations, the influence of global warming on the temperature extremes over China under the Paris Agreement targets has been investigated in this study. Our major findings are summarized as follows:

The rapid increases in global mean temperature with respect to pre-industrial levels are projected to drive changes in the magnitude and occurrence probability of temperature extremes. While the spatial patterns of PR are very similar for a climate variable with specific return level, there are substantial differences in the PR between the two global warming levels and also the different recurrence periods. For example, the PR of once-in-100-year TXx and TNx events are 14.4 and 31.4 at 1.5 °C warming, which transfer to the return periods of 7 and 2 years. However, under 2 °C global warming, once-in-100-year TXx and TNx events are projected to occur about every 5 and 2 years (the risks are 23.3 and 50.6), respectively.

Changes in probability ratios reflect the behavior of shifting location and changing variability of a GEV distribution. The risks in the Tibetan Plateau and south of the Yangtze River are higher due to their sensitivity to location and scale parameters, with once-in-20-year TXx projected to increase by more than 5 (0.25) and 3 (0.75) times under 2 °C warming over these two regions, respectively, as a result of the greater warming amplitude (increased variability). Risks for regions with decreased variability (i.e., Northwest China for TXx, the Tibetan Plateau and Northwest China for TNx) appear to be straightforwardly affected by the behavior of location parameter, which transfers to more than 3, 6 and 4 times increase in the PR relative to the historical climate. For TNx, regions with weaker warming and increased variability (i.e., Northeast China), the risks are also closely associated with the combined effect of location parameter and changing variability. Furthermore, compared with TXx, the smaller variability of TNx results in a greater change in the probability for a specific warming level.

Our results highlight that there are substantial differences in the risks of temperature extremes between the 1.5 °C and 2 °C global warming levels, which has a strong implication for climate change adaptation strategies over China. The complex changes of temperature distributions can induce large effects on the risks of temperature extremes. Also, physical processes (i.e., soil−moisture−climate interaction) are important for understanding the changes in temperature extremes, though we did not explore them in this study.

Declaration of competing interest

The authors declare no conflict of interest.

Acknowledgments

This research is supported by the National Key Research and Development Program of China (2017YFA0603804 and 2016YFA0600402). We would like to acknowledge the World Climate Research Programme's Working Group on Coupled Modelling, which is responsible for CMIP and we thank the climate modeling groups for producing and making their model outputs available.

References

Coles, S., 2001. An Introduction to Statistical Modeling of Extreme Values. Springer, London.

Donat, M.G., Alexander, L.V., 2012. The shifting probability distribution of global daytime and night-time temperatures. Geophys. Res. Lett. 39 (14), L14707.

Easterling, D.R., Meehl, G.A., Parmesan, C., et al., 2000. Climate extremes: observations, modeling, and impacts. Science 289 (5487), 2068−2074.

Fischer, E.M., Knutti, R., 2015. Anthropogenic contribution to global occurrence of heavy-precipitation and high-temperature extremes. Nat. Clim. Change 5 (6), 560−564.

Frölicher, T.L., Laufkötter, C., 2018. Emerging risks from marine heat waves. Nat. Commun. 9 (1), 650.

Fu, Y., Lu, R., Guo, D., 2018. Changes in surface air temperature over China under the 1.5 and 2.0°C global warming targets. Adv. Clim. Change Res. 9 (2), 112−119.

Goubanova, K., Li, L., 2007. Extremes in temperature and precipitation around the Mediterranean basin in an ensemble of future climate scenario simulations. Global Planet. Change 57, 27−42.

Guo, L., Jiang, Z., Chen, W., et al., 2018. Bias correction and projection of surface air temperature in LMDZ multiple simulation over central and eastern China. Adv. Clim. Change Res. 9 (1), 81−92.

Guo, L., Jiang, Z., Ding, M., et al., 2019. Downscaling and projection of summer rainfall in eastern China using a nonhomogeneous hidden Markov model. Int. J. Climatol. 39 (3), 1319−1330.

Guo, L., Jiang, Z., Chen, D., et al., 2020. Projected precipitation changes over China for global warming levels at 1.5 °C and 2 °C in an ensemble of regional climate simulations: impact of bias correction methods. Clim. Change 1−21. https://doi.org/10.1007/s10584-020-02841-z.

Huang, J., Liu, Y., Ma, L., et al., 2013. Methodology for the assessment and classification of regional vulnerability to natural hazards in China: the application of a DEA model. Nat. Hazards 65 (1), 115−134.

Huang, W.K., Stein, M.L., McInerney, D.J., et al., 2016. Estimating changes in temperature extremes from millennial scale climate simulations using generalized extreme value (GEV) distributions. Adv. Stat. Climatol. Meteorol. Oceanogr. 2, 79−103.

IPCC, 2013. Climate Change 2013: The Physical Science Basis. Contribution of Working Group I to Fifth Assessment Report of the Intergovernmental Panel on Climate Change. Cambridge University Press, Cambridge and New York.

Jiang, D., Fu, Y., 2012. Climate change over China with a 2°C global warming. Chin. J. Atmos. Sci. 36 (2), 234−246 (in Chinese).

Jiang, D., Zhang, Y., Sun, J., 2009. Ensemble projection of 1–3°C warming in China. Chin. Sci. Bull. 54 (18), 3326−3334.

Kharin, V.V., Zwiers, F.W., Zhang, X., et al., 2007. Changes in temperature and precipitation extremes in the IPCC ensemble of global coupled model simulations. J. Clim. 20 (8), 1419−1444.

Kharin, V.V., Zwiers, F.W., Zhang, X., et al., 2013. Changes in temperature and precipitation extremes in the CMIP5 ensemble. Clim. Change 119 (2), 345−357.

Kharin, V.V., Flato, G.M., Zhang, X., et al., 2018. Risks from climate extremes change differently from 1.5°C to 2.0°C depending on rarity. Earths Future 6, 704−715.

Knutti, R., Rogelj, J., Sedláček, J., et al., 2016. A scientific critique of the two-degree climate change target. Nat. Geosci. 9 (1), 13−18.

Lang, X., Sui, Y., 2013. Changes in mean and extreme climates over China with a 2°C global warming. Chin. Sci. Bull. 58 (12), 1453−1461.

Lee, J., Li, S., Lund, R., 2014. Trends in extreme US temperatures. J. Clim. 27 (11), 4209−4225.

Li, M., Jiang, Z., Zhou, P., et al., 2020. Projection and possible causes of summer precipitation in eastern China using self-organizing map. Clim. Dynam. 54, 2815−2830.

Li, W., Jiang, Z., Zhang, X., et al., 2018a. On the emergence of anthropogenic signal in extreme precipitation change over China. Geophys. Res. Lett. 45 (17), 9179−9185.

Li, W., Jiang, Z., Zhang, X., et al., 2018b. Additional risk in extreme precipitation in China from 1.5°C to 2.0°C global warming levels. Sci. Bull. 63 (4), 228−234.

McKinnon, K.A., Rhines, A., Tingley, M.P., et al., 2016. The changing shape of Northern Hemisphere summer temperature distributions. J. Geophys. Res. Atmos. 121 (15), 8849−8868.

Parey, S., Hoang, T.T.H., Dacunha-Castelle, D., 2013. The importance of mean and variance in predicting changes in temperature extremes. J. Geophys. Res. Atmos. 118 (15), 8285−8296.

Peters, G.P., Andrew, R.M., Boden, T., et al., 2013. The challenge to keep global warming below 2°C. Nat. Clim. Change 3 (1), 4−6.

Rhines, A., Huybers, P., 2013. Frequent summer temperature extremes reflect changes in the mean, not the variance. Proc. Natl. Acad. Sci. U. S. A. 110 (7), E546.

Shi, C., Jiang, Z., Chen, W., et al., 2018. Changes in temperature extremes over China under 1.5°C and 2°C global warming targets. Adv. Clim. Change Res. 9 (2), 120−129.

Stott, P.A., Stone, D.A., Allen, M.R., 2004. Human contribution to the European heatwave of 2003. Nature 432 (7017), 610.

Stott, P.A., Christidis, N., Otto, F.E., et al., 2016. Attribution of extreme weather and climate-related events. Wiley Interdiscip. Rev. Clim. Change 7 (1), 23−41.

Sui, Y., Lang, X., Jiang, D., 2015. Temperature and precipitation signals over China with a 2°C global warming. Clim. Res. 64 (3), 227−242.

Sui, Y., Lang, X., Jiang, D., 2018. Projected signals in climate extremes over China associated with a 2°C global warming under two RCP scenarios. Int. J. Climatol. 38, e678−e697.

Sun, C., Jiang, Z., Li, W., et al., 2019. Changes in extreme temperature over China when global warming stabilized at 1.5°C and 2.0°C. Sci. Rep. 9 (1), 1−11.

Sun, Y., Hu, T., Zhang, X., 2018. Substantial increase in heat wave risks in China in a future warmer world. Earths Future 6, 1528−1538.

Sun, Y., Song, L., Yin, H., et al., 2016. Human influence on the 2015 extreme high temperature events in Western China. Bull. Am. Meteorol. Soc. 97 (12), S102−S106.

UNFCCC, 2015. Adoption of the Paris Agreement. Proposal by the President. Report No.FCCC/CP/2015/L.9/Rev.1. https://unfccc.int/sites/default/files/resource/docs/2015/cop21/eng/l09r01.pdf.

WMO, 2020. WMO statement on the state of the global climate in 2019. Available online. https://public.wmo.int/en/our-mandate/climate/wmo-statement-state-of-global-climate.

Yin, S.Y., Wang, T., Hua, W., et al., 2020. Mid-summer surface air temperature and its internal variability over China at 1.5 °C and 2 °C of global warming. Adv. Clim. Change Res. 11 (3), 185−197. https://doi.org/10.1016/j.accre.2020.09.005.

Yu, R., Zhai, P., Lu, Y., 2018. Implications of differential effects between 1.5 and 2°C global warming on temperature and precipitation extremes in China's urban agglomerations. Int. J. Climatol. 38 (5), 2374−2385.

Zhang, G., Zeng, G., Vedaste, I., et al., 2020. Regional changes in extreme heat events in China under stabilized 1.5°C and 2.0°C global warming. Adv. Clim. Change Res. 11 (3), 198−209. https://doi.org/10.1016/j.accre.2020.08.003.

Zhang, X., Alexander, L., Hegerl, G.C., et al., 2011. Indices for monitoring changes in extremes based on daily temperature and precipitation data.

Wiley Interdiscip. Rev. Clim. Change 2 (6), 851−870. https://doi.org/10.1016/j.accre.2020.08.003.

Zhang, Y., Gao, Z., Pan, Z., et al., 2017. Spatiotemporal variability of extreme temperature frequency and amplitude in China. Atmos. Res. 185, 131−141.

Zhu, L., Li, Y., Jiang, Z., 2017. Statistical modeling of CMIP5 projected changes in extreme wet spells over China in the late 21st century. J. Meteor. Res. 31 (4), 678−693.